Available online at www.sciencedirect.com

ScienceDirect

Biomedical Journal

journal homepage: www.elsevier.com/locate/bj

Original Article

Topological properties and *in vitro* identification of essential nodes of the Paclitaxel and Vincristine interactomes in PC-3 cells

Claudia Delgado-Carreño [a,b], *Gina Méndez-Callejas* [a,*]

[a] *Group of Biomedical Research and Applied Human Genetics, Laboratory of Cellular and Molecular Biology, School of Medicine, University of Applied and Environmental Sciences, U.D.C.A, Bogota, Colombia*
[b] *Department of Chemistry, Faculty of Science, Javeriana University, Bogota, Colombia*

ARTICLE INFO

Article history:
Received 6 June 2018
Accepted 12 April 2019
Available online 31 October 2019

Keywords:
Prostate cancer
Interactome
Essential nodes
Microtubule-targeting agents (MTAs)
Apoptotic proteins

ABSTRACT

Background: Microtubule-targeting agents (MTAs) disrupt microtubule dynamics, thereby inducing apoptosis via mitochondrial pathway activation through the modulation in the expression of the Bcl-2 family.
Methods: To describe topological features of the MTAs networks associated to intrinsic apoptosis induction in p53-null prostate cancer cells, we predicted and compared the interactomes and topological properties of Paclitaxel and Vincristine, and thus, the essential nodes corresponding with the pro- and anti-apoptotic proteins and their kinetics were subjected to experimental analysis in PC-3 cell line.
Results: The essential nodes of the apoptotic pathways, TP53, and CASP3, were identified in both, Paclitaxel and Vincristine networks, but the intrinsic pathway markers BCL2, BAX, and BCL2L1 were identified as hub nodes only in the Paclitaxel network. An *in vitro* analysis demonstrated an increase in BimEL and the cleaved-caspase-3 proteins in PC-3 cells exposed to both treatments. Immunoprecipitation analysis showed that treatments induced the releasing of Bax from the anti-apoptotic complex with Bcl-2 protein and the role of BimEL as a de-repressor from sequestering complexes, in addition, new protein complexes were identified between BimEL or Bcl-2 and cleaved-caspase-3, contributing data to the Vincristine network for p53-null cells in response to MTAs.
Conclusion: The differences in sensitivities, protein profiles, and protein complex kinetics observed between the drugs confirmed that the selectivity and stimulation of the apoptotic system vary depending on the cell's genotype, the drug used and its exposure period.

* *Corresponding author*. School of Medicine, University of Applied and Environmental Sciences, U.D.C.A, 222 street # 55-37, 111166, Bogota, Colombia.
E-mail address: gmendez@udca.edu.co (G. Méndez-Callejas).
Peer review under responsibility of Chang Gung University.
https://doi.org/10.1016/j.bj.2019.04.003

At a glance commentary

Scientific background on the subject

Cancer is a significant cause of morbidity and mortality of the world population, being the first cause of non-violent death. Prostatic cancer has become the most common malignancy among men. Network biology with an experimental approach can be used to described protein interaction, identify biomarkers and define the topological features of cytostatic drugs among other uses.

What this study adds to the field

Advance and variant forms of prostatic cancer are not susceptible to common treatment which leads to the pursuit of different classes of drugs, such as MTAs, in which the resistance rate and protein interaction between drugs vary. Some protein interactions were previously described by network biology and then verified in this paper, also, new interactions were found.

Network biology has been extensively used to describe how proteins interact and coordinate cellular responses [1]. Protein–protein network approaches have been applied to gain a better understanding of cancer mechanisms [2], to identify cancer subnetworks [3], to discover cancer-related biomarkers [4], and to define the topological features of the interactome of microtubule-targeting agents (MTAs) [5].

High cancer death rates and resistance or over-sensitivity to conventional cancer therapies remain major challenges for researchers [6,7]. Prostate cancer has become the most common malignancy among men and is the second leading cause of cancer death worldwide [8,9]. Prostate cancer is very heterogeneous, often characterized by the presence of AR-dependent and AR-independent cellular clones in the same patient [10], its biological, hormonal, and molecular characteristics are extremely complex [6].

Most prostatic cancers (PCs) are adenocarcinomas characterized by a glandular formation, lack of basal cells, uncontrolled proliferation of malignant tumor cells and the expression of androgen receptor (AR) and prostate-specific antigen (PSA). These adenocarcinomas are indolent and androgen-dependent (AD) [6], although localized PC may be successfully treated with radical prostatectomy and external beam radiation, many patients subsequently develop metastatic disease. Since its growth is driven by androgens, they are primarily treated with hormonal therapy, the androgen ablation therapy (ADT), that aims to block or decrease the expression of the androgen receptor, the hormonal therapy is the standard treatment of hormone-naïve metastatic disease [11–13]. Nearly all patients with metastatic prostate cancer (PC) become resistant to the initial approach with ADT, developing the state known as metastatic castration-resistant prostate cancer (mCRPC) [10].

There are variant forms of prostatic epithelial malignancies, such the Small-Cell Neuroendocrine Carcinoma (SCNC), which are rare tumors that account for no more than 1% of all carcinomas of the prostate, they lack AR and PSA expression. Although they may arise de novo, they are often seen as recurrent tumors in patients who have received hormonal therapy with conventional prostatic adenocarcinoma [6]. PC-3 is a cell line characteristic of SCNC since PC-3 cells share a lot of traits with prostatic SCNCs, including the lack of expression of the basal markers AR and PSA. PC-3 cells are often referred to as aggressive, androgen-independent (AI), and castration-resistant [6,14]. Nevertheless, the PC-3 line presents a base deletion at codon 138 (GCC→GC) in the *TP53* gene, resulting in a frame-shift mutation [15,16] that influences negatively p53 dependent-apoptosis through the mitochondrial pathway, where it directly interact with different Bcl2 family members, acting as a direct activator of the Bax/Bak effectors, or as a sensitizer/de-repressor of Bcl-x/2 and Mcl-1 [17]. In human cancers, TP53 gene is frequently mutated what not only leads to loss of its tumor suppressive function but also acquires dominant–negative activities and gains new oncogenic properties that increase drug resistance [14,18,19].

Advanced and variants forms of these PCs are only temporary or not susceptible at all to the androgen ablation therapy, leading to the pursuit of different classes of drugs, such as MTAs, which inhibit microtubule dynamics and induce cell death via the mitochondrial intrinsic pathway [12,20].

Microtubule-targeting agents are usually obtained from natural sources, such as Paclitaxel, obtained from the Pacific yew tree (*Taxus brevifolia*) [8], and Vincristine, obtained from Madagascar periwinkle (*Catharanthus roseus*) [21]. These agents disrupt microtubules dynamics, thereby inducing apoptosis via mitochondrial pathway activation [19]. Prostate cancer exhibits high levels of anti-apoptotic Bcl-2 and Bcl-xL proteins in refractory and advanced disease, contributing to the defective apoptosis associated with poor prognosis, treatment resistance and disease progression [8,12,22–24].

The mitotic arrest is induced by two kinds of well-known MTAs, including the microtubule-stabilizing agent Paclitaxel [25] and microtubule-destabilizing agents, such as Vincristine and Vinblastine [26], which are associated with the activation of Raf-1 protein kinase and the phosphorylation of the anti-apoptotic protein Bcl-2 [25]. This phosphorylation increases the resistance to many anticancer drugs and may inactivate the Bcl-2 protein, ensuring cell death after microtubule rupture and DNA fragmentation in PC-3 cells [25,26]; additionally, it inhibits the ability of Bcl-2 to interfere with pro-apoptotic proteins, such as Bax, leading to apoptosis [22]. Paclitaxel also induces the accumulation of the pro-apoptotic protein Bim [12], causing a G2/M cell cycle block, mitochondria damage, and p53-independent apoptosis [27].

Activation of the caspase cascade has been correlated with the outset of apoptosis [28]. Caspase inhibition attenuates apoptosis in prostate cancer cells in response to diverse apoptotic stimuli, including androgen ablation. Therefore, reduced caspase expression, which is a frequent event in

prostatic cancer, has been linked with poor prognosis and/or resistance to therapy in several human tumors. Caspases-1, -3, and -9 are the three key caspases implicated in the execution of apoptosis in prostate cancer cells and malignant prostatic tissue, and there is dramatically reduced caspase-1 and -3 immunoreactivity among the tumor cells [29].

The secondary targets of the signaling pathways induced by Paclitaxel and Vincristine in PC-3 cancer cells remain poorly understood. Here, we described the topological properties and identified the essential nodes of Paclitaxel and Vincristine interactomes against the human proteome. Then, experimental validation of those essential nodes, corresponding to pro- and anti-apoptotic proteins and their kinetics in p53-null PC-3 cancer cells in regard to the intrinsic apoptosis induced by Paclitaxel and Vincristine was conducted.

Materials and methods

Paclitaxel and Vincristine network prediction

The chemical information of Paclitaxel and Vincristine was extracted from the PubChem database. After, the interaction between proteins and the MTAs were integrated into a network by using of the Search Tool for Interacting Chemicals (STICH) 5.0 database [30] (http://stitch.embl.de/), with the following criteria: a confidence score of 0.500, with a maximum of 500 interactions. The prediction methods in the program were active solely against the human proteome. Next, each network was imported into Cytoscape 3.4.0 [31], and the following topological parameters were obtained: Degree (k), which indicates the connection density of each node; Betweenness Centrality (BC), which indicates the number of times a node is visited; Closeness Centrality (CC), which indicates what nodes are closer to the center of the network; and Stress, which indicates how many times a particular node is part of different shortest paths using the Network Analyzer plugin included by default in Cytoscape.

To determine the functional richness of the network, a hypergeometric distribution was used and the false discovery rate (FDR) correction was included, using the Biological Network Gene Ontology (BiNGO) plugin. The FDR correction, with a significance level of 0.05, is shown for two descriptive categories of the clusters. The first represents the biological function, and the second represents node mapping in the Kyoto Encyclopedia of Genes and Genomes (KEGG) [32].

Compounds, cell lines, and culture conditions

The Paclitaxel and Vincristine sulfate (Cayman Chemical) was dissolved in dimethyl sulfoxide (DMSO) and for the experiments, dilutions were made in supplemented Eagle's Minimum Essential Medium (EMEM) with 10% (w/v) Fetal Bovine Serum (Biowest), 2 mM L-glutamine, 5000 UI/ml penicillin and 5 mg/ml streptomycin. The prostate adenocarcinoma PC-3 cells (ATCC® CRL1435™) were grown in supplemented EMEM at 37 °C in a humidified atmosphere containing 5% CO_2.

The 3-(4,5-methyl-thiazol-2-yl)-2,5-diphenyl-tetrazolium bromide (MTT) cell viability assay

PC-3 cells were cultured to 80% confluence, then, seven thousand cells approximately were seeded per well in a 96-well plate and were grown at 37 °C, 5% CO_2 for 24 h. Then, MTAs treatments were administered at different concentrations, between 0,01 and 0.15 μg/mL for Vincristine and between 0.005, and 0,0012 μg/mL for Paclitaxel. Incubation was carried out for 48 h. Following the incubation time, 100 μl of 0.5 mg/mL of the MTT solution, dissolved in a medium without phenol red, were added and incubated for 4 h. Formazan crystals were dissolved with 100 μl of DMSO. The results were determined by the optical density (OD) determined by the absorbance at 570 nm [33]. Estimation of the MTAs concentrations required to reduce the 50% of cell viability (IC_{50}) was done using nonlinear regression from plotting cell survival (%) versus drug concentration [μg/mL].

Immunofluorescence analysis

Seven thousand PC-3 cells approximately were seeded per well in a 96-well plate and were grown for 24 h before treatment. The cells were treated with Paclitaxel and Vincristine at the IC_{50} and incubated for 24 h. Later the cells were fixed in methanol (−20 °C), and then with acetone at −20 °C for 20 s. The microtubules were stained with anti-α-tubulin monoclonal antibody DM1A (Sigma–Aldrich) and goat anti-mouse Alexa Fluor 488 (Molecular Probes), both diluted in 5% BSA/TTBS (w/v) blocking solution. DNA staining was done with 1.0 μg/mL of DAPI (Invitrogen) [22,33]. Fluorescence was monitored using an epifluorescence microscope (Motic AE31), and the images were captured with the MoticCamPro 282A and analyzed with Motic Image plus 2.0 software.

Electrophoresis & western blotting

Protein extraction was carried out from approximately 6 million cells treated for 6, 16, 24 and 48 h with the MTAs at the corresponding IC_{50} using a lysis buffer (Tris HCl pH 8.0 20 mM, NaCl 137 mM, Glycerol 10%, Np40 1%, EDTA 10 mM) [34], and the protein concentration was determined by Bicinchoninic Acid (BCA) Protein Assay Kit (Pierce). Fifteen μg of protein were subjected to an 11% SDS-PAGE gel electrophoresis using a mini-gel system (Protean II; Bio-Rad Laboratories). Proteins were blotted using polyvinylidene fluoride (PVDF) membranes [35,36]. The transferred membranes were blocked in 5% (w/v) BSA/TTBS followed by overnight incubation with the following primary antibodies: anti-α-Tubulin (Sigma–Aldrich); anti-Bim; anti-Bax; anti-Bcl-2 (Gene-Tex); anti-procaspase-3 (Novus) or anti-caspase-3 (Thermo-Fisher Scientific). Next, the membranes were incubated with the correspondent secondary antibody, either anti-mouse IgG (Sigma–Aldrich) or anti-rabbit IgG (Cell Signaling), for 1 h at room temperature. The bands were visualized using a Chemiluminescent Detection System (Thermo-Fisher Scientific) [22]. Image J software was used to quantify and compare the density of bands [37].

Co-immunoprecipitation

One-hundred and fifty μg of protein per treatment were mixed with 2ug of primary antibody, in a dilution buffer −NaCl (Tris HCl pH 7.4, EDTA 10 nM, NP40 1%, NaF 50 mM, PMSF 1 mM, and protease inhibitors cocktail (Pierce) (Thermo Fisher Scientific) 1:100), and the samples were incubated at 4 °C for 4 h. Later, the protein mix was incubated with the washed resin (Protein G) (Thermo-Fisher Scientific) at 4 °C overnight. The next day, the samples were washed with a +NaCl wash buffer (Tris HCl pH 7.4 1 M, NaCl, EDTA 10 mM, NP40 1%, NaF 50 mM, PMSF 1 mM and protease inhibitors cocktail (Pierce) (Thermo Fisher Scientific) 1:100) and were reduced with 35 μl of a 1x loading buffer and boiling for 5 min. Subsequently, the immunoprecipitated complexes were subjected to electrophoresis and western blotting with primary antibodies against the corresponding essential nodes from intrinsic apoptosis pathway, the detection of the proteins in the complex was conducted as previously described and densitometry analyses were performed using ImageJ software [37].

Results

Topological nodes that regulate the Paclitaxel and Vincristine interactomes

The Paclitaxel and Vincristine interactomes showed several secondary targets [Fig. 1]. The Paclitaxel network presented 166 nodes and 1497 edges. The evaluated topological features showed positive correlations, indicative of highly connected nodes, as follows: nodes/k (R: 0.857, R^2: 0.657); neighbors/BC (R: 0.972, R^2: 0.871) and neighbors/CC (R: 0.767, R^2: 0.592) [Fig. 1A]. Then, to choose the essential nodes, the k values were reordered in a decreasing fashion, and the top 30 nodes with the highest values are showed [Table 1]. To determine the importance of the essential nodes during the process the information flow in the network, a linear correlation analysis between the BC and stress parameters was conducted. The essential nodes TP53, AKT1, VEGFA, JUN, and CASP3 seemed to control the information processing in the paclitaxel

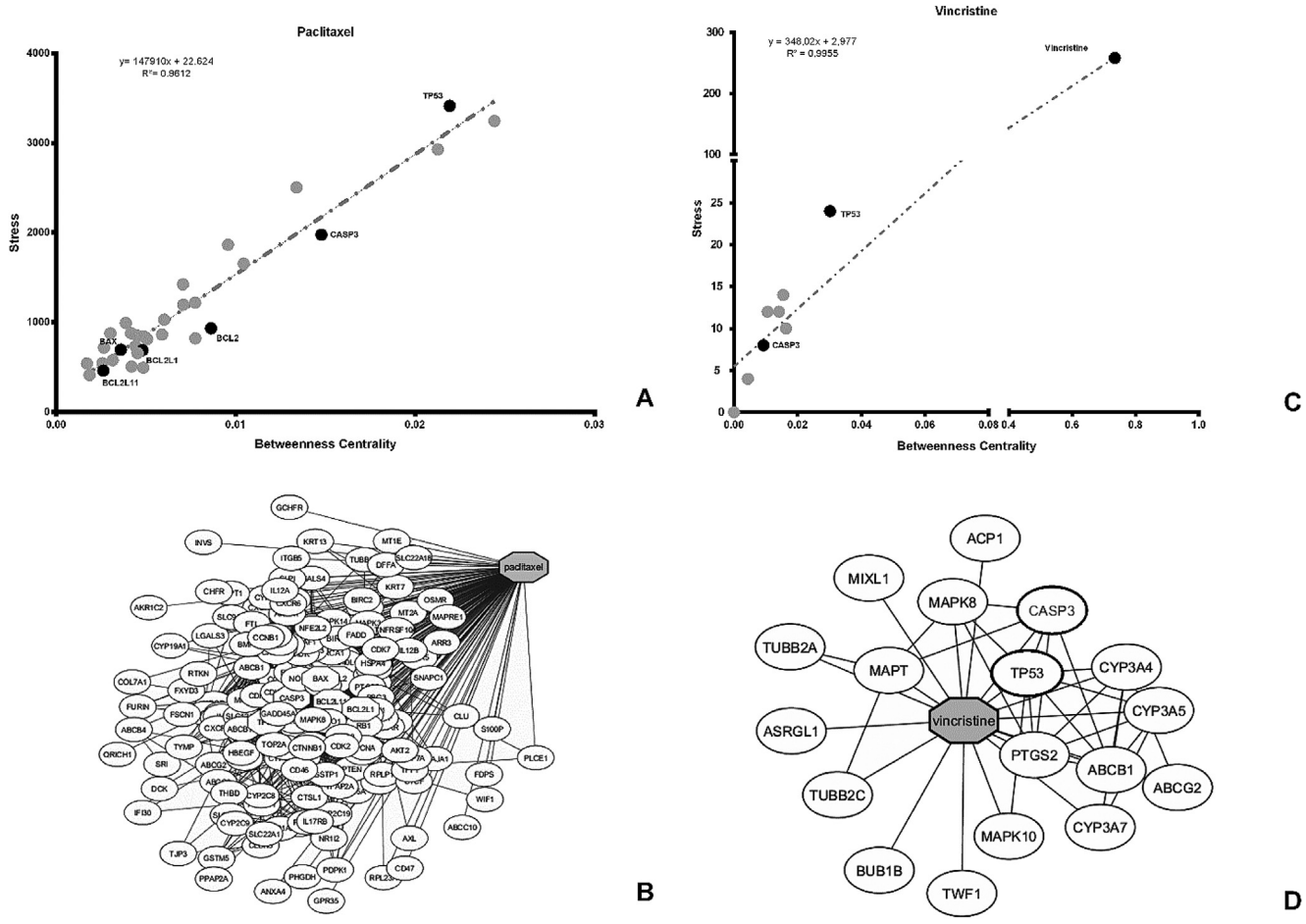

Fig. 1 Topological nodes that regulate the interactome information process derived from Paclitaxel and Vincristine. (A, C) Stress and BC values were used to identify the nodes that connect the most significant shortest in the interactomes and thus, define how the information flow is distributed. (B, D) The essential interactomes were built based of the K parameter and shows the most connected nodes in both interactomes.

Table 1 Essential topological nodes from Paclitaxel and Vincristine networks based on the k parameter.

Node	k	BC	CC
Paclitaxel	165	0.621	1.000
TP53	74	0.022	0.645
AKT1	71	0.024	0.637
VEGFA	68	0.021	0.630
JUN	66	0.013	0.625
CASP3	60	0.010	0.611
EGFR	58	0.015	0.607
PTGS2	55	0.010	0.600
MAPK1	52	0.007	0.594
STAT3	50	0.008	0.589
CASP8	49	0.004	0.587
ERBB2	49	0.007	0.587
CDKN1A	47	0.003	0.583
CYCS	46	0.004	0.581
BIRC5	45	0.004	0.579
MAPK8	45	0.006	0.579
PARP1	45	0.005	0.579
PCNA	44	0.009	0.577
FASLG	44	0.005	0.577
BCL2	43	0.003	0.575
PIK3CA	43	0.006	0.575
PTEN	42	0.004	0.573
BAX	41	0.002	0.571
CDH1	40	0.008	0.569
MAPK14	39	0.004	0.567
MDM2	39	0.003	0.567
SOD2	37	0.005	0.563
BCL2L1	37	0.003	0.563
IL8	36	0.005	0.561
Vincristine	18	0.735	1.000
TP53	8	0.030	0.643
PTGS2	7	0.011	0.621
ABCB1	7	0.015	0.621
CASP3	6	0.009	0.600
CYP3A4	6	0.014	0.600
MAPK8	5	0.004	0.581
MAPT	5	0.016	0.581
CYP3A5	5	0.007	0.581
ABCG2	3	0.000	0.545
CYP3A7	3	0.001	0.545
MAPK10	2	0.000	0.529
TUBB2C	2	0.000	0.529
TUBB2A	2	0.000	0.529
BUB1B	1	0.000	0.514
ASRGL1	1	0.000	0.514
ACP1	1	0.000	0.514
MIXL1	1	0.000	0.514
TWF1	1	0.000	0.514

network [Fig. 1B], but also in the top the BCL 2, BAX and BCL2L1 nodes were identified confirming the mitochondrial-mediated pathway apoptosis induction.

The Vincristine network presented 19 nodes and 42 edges. This network also reveals essential nodes and highly significant correlations were detected among their basic topological parameters as follows: nodes/k (R: 0.913, R^2: 0.770); neighbors/BC (R: 0.999, R^2: 0.926) and neighbors/CC (R: 0.807, R^2: 0.695) [Fig. 1C], and only two essential nodes, TP53 and CASP3, associated to the intrinsic apoptosis, seems to be involved in the information processing of the network [Fig. 1D].

Paclitaxel and Vincristine cause irreversible morphologic damage in PC-3 cells

Vincristine and Paclitaxel inhibitory effect on PC-3 cells proliferation was confirmed by MTT assay. However, the IC_{50} values demonstrated that the cells were significantly more sensitive to Paclitaxel [2.81 nM] than to Vincristine [44,8 nM] [Fig. 2]. Those IC_{50} data were used for all others *in vitro* analyses.

Morphological analysis was performed to examine the cellular damage that occurred after exposing PC-3 cells to MTAs using immunofluorescence microscopy [Fig. 3A]. There were variations in the cells on the morphological scale, such as microtubule and nucleus integrity and cell shape and size variations. Paclitaxel mainly affects the microtubules, causing microtubule destabilization, and increase in cytosol size, the appearance of some apoptotic bodies (marked with a red arrow), and the emergence of different nuclear morphologies [Fig. 3A]. On the other hand, the Vincristine effect on cell proliferation was more evident than paclitaxel and the cells had dense and compact damaged microtubules around the nuclei, and, thus some apoptotic cells (marked with a red arrowhead). The nuclei of PC-3 cells exposed to Vincristine had irregular and small nuclei compared to the control but not as quite as paclitaxel. Further, Paclitaxel-induced the condensation and fragmentation of the nuclear material (in blue) as well as a reduction of its perimeter [Fig. 3B].

Role of Paclitaxel and Vincristine treatments in the expression of essential node proteins in PC-3 cells

The content of the essential nodes, the Bcl-2, Bim, Bax, procaspase-3 and cleaved-caspase-3 proteins, was evaluated by western blot at 0, 6, 16, 24 and 48 h of treatments with Paclitaxel and Vincristine. Both drugs stimulated an increase in the expression of Bim protein [Fig. 4A], and caused a significant decrease in the level of anti-apoptotic protein Bcl-2, leading the way for apoptosis. But the effects on Bax, procaspase-3 and cleaved caspase-3 proteins,

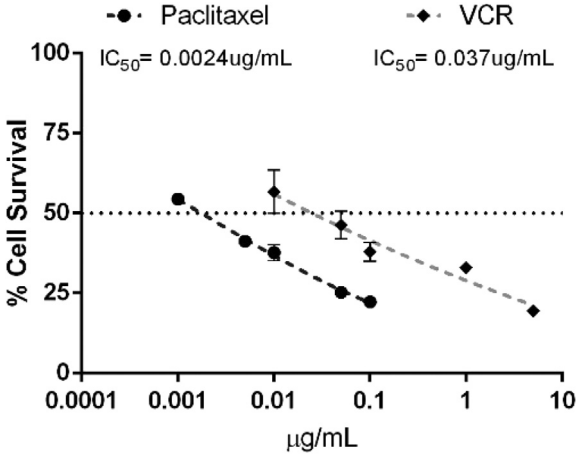

Fig. 2 Percentage of cell viability of PC-3 cells exposed to different concentrations of Paclitaxel and Vincristine. The inhibitory concentration of cell viability (IC_{50}) was calculated by non-linear regression using Graph Pad 6.0 software.

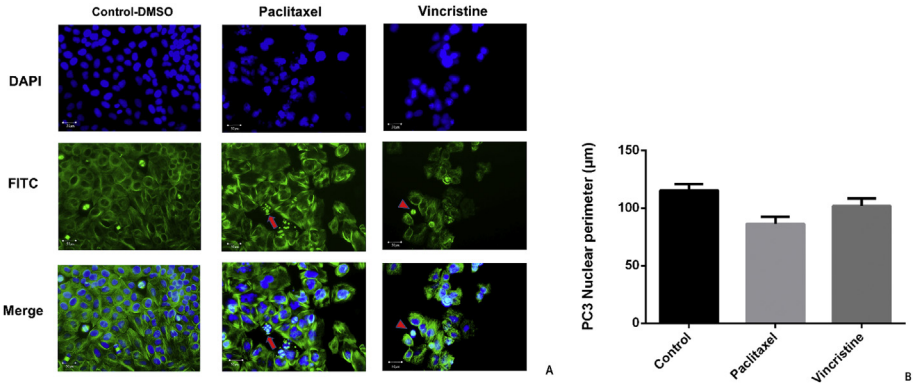

Fig. 3 Morphological changes in PC-3. (A) Immunofluorescence micrograph showing the nuclear (in blue) and microtubular (in green) effects in PC-3 cancer cells after 24 h of incubation with two microtubule-targeting agents, Vincristine and Paclitaxel. (B) The nuclear perimeter of PC-3 cells before and after being treated with the MTAs Paclitaxel and Vincristine. Motic 2.0 software was used to measure the nuclei.

were divergent between the two drugs. Paclitaxel-induced a slight decrease in the levels of Bax protein, which was dependent on time, while Vincristine caused an increase through a distinct period of the drug incubation. Paclitaxel did not provoke considerable changes in the levels of the procaspase-3 form, but the active form was slightly augmented. Furthermore, in the cells treated with Vincristine, there was a decrease in the levels of procaspase-3 at 48 h, which was related with the decrease in the expression of the activated form that was observed at the same time [Fig. 4B].

In vitro *protein–protein interactions in PC-3 cells after Paclitaxel and Vincristine treatment*

Immunoprecipitation analyses showed that Bim protein interacted with the essential nodes Bcl-2, Bax and cleaved-caspase-3. However, the intensity of the bands indicated that the function of Bim was dependent on the type of drug [Fig. 5A]. The Bim/Bcl-2 interaction was similar in both treatments, decreasing slightly at 48 h. Bim/Bax complex levels increased significantly at 16 h only in the cells exposed to Paclitaxel. Interestingly, new interactions have been identified in cells that were exposed to vincristine, since there was an augmentation in the interaction between Bim/cleaved-caspase-3 in a time-dependent manner [Fig. 5B].

The Bcl-2/Bax interaction was significantly decreased at 48 h treatment in cells exposed to Paclitaxel [Fig. 5A and B]. In contrast, in cells exposed to Vincristine, the Bax protein has not been completely released at 48 h from the anti-apoptotic complex, elucidating the PC-3 mechanism to Vincristine resistance. Another new protein–protein interaction was revealed between cleaved-caspase-3 and Bcl-2,

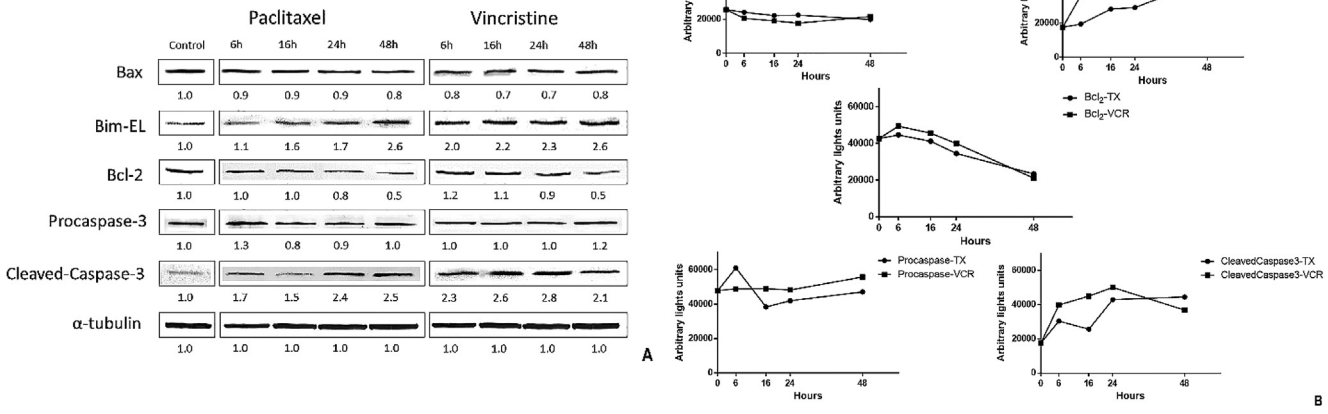

Fig. 4 Comparison between the pro-apoptotic and anti-apoptotic protein levels in PC-3 cells treated for up to 48 h with two MTAs, Paclitaxel, and Vincristine. (A) The readouts, defined as the protein complex levels, were normalized to the readouts of α-tubulin, which are shown below each band. (B) The immunoblot images were quantitated by ImageJ and were then graphed using GraphPad Prism 6. The readouts, defined as the arbitrary light units of the pro-apoptotic and antiapoptotic proteins, are the relative densitometric units of each band.

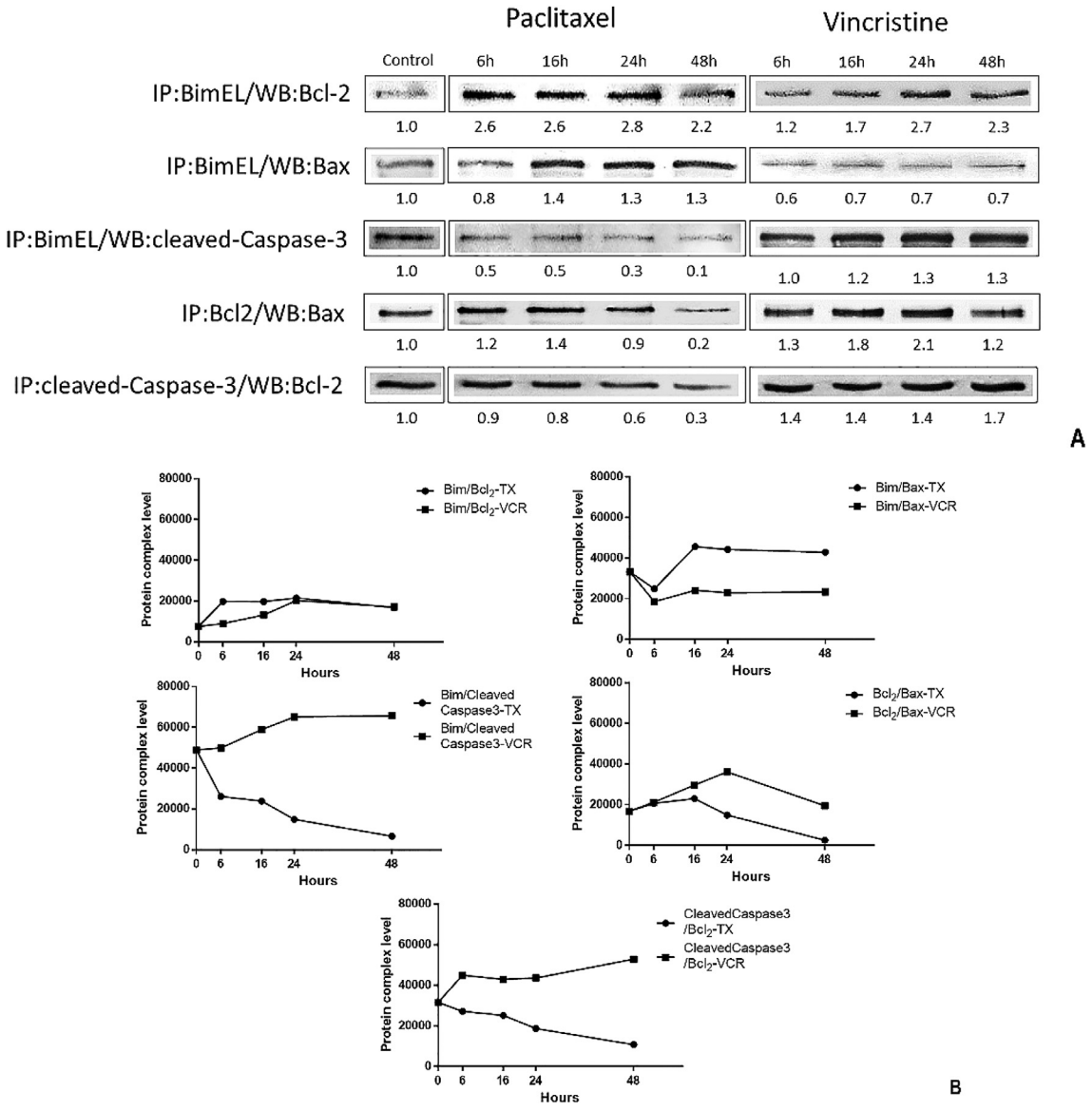

Fig. 5 Comparison between immunocomplex interactions in PC-3 cells treated for up to 48 h with two MTAs, Paclitaxel, and Vincristine. (A) The readouts, defined as the protein complex levels, were normalized to the readouts of α-tubulin, which are shown below each band. (B) The immunoblot images were quantitated by ImageJ and were then graphed using GraphPad Prism 6. The readouts, defined as the levels of the complexes of the pro-apoptotic and antiapoptotic proteins, were the relative densitometric units of each band.

where the levels of this complex decreased in the cells treated with Paclitaxel and increased after Vincristine treatment, much like the levels of the Bim/cleaved-caspase-3 complex [Fig. 5B].

Discussion

Paclitaxel and Vincristine bind preferentially and reversibly to the β-tubulin microtubule subunit, promoting the polymerization or depolymerization of microtubules, respectively; both drugs disrupt microtubule dynamics [38]. However, the networks here predicted show several secondary targets, indicating their lack of specificity. The Paclitaxel interactome was more highly expressed than the Vincristine interactome and presented more pro- and anti-apoptotic proteins, suggesting that this compound has pleiotropic moieties possibly related to unspecific cellular activation and the regulation of cell death and toxicity. The Vincristine network was more specific towards activated proteins that regulate the induction of cell death. According to preliminary computational results, we observed that Paclitaxel has significant druggability towards Bax, Bcl-2, and cleaved-caspase-3, indicating that this molecule can induce non-regulated biochemical signaling, and stimulate an apoptotic catastrophe [39] and even induce paraptosis [Fig. 1] [40].

The prostate cancer cell line PC-3 is an appropriate model to study the possible causes of the ineffectiveness of the common

drugs used in the treatment of apoptosis-resistant phenotypes cells with p53-null status, which alter the normal function of the network determinants for each drug [Fig. 1]. Previously, it was showed that PC-3 cells exposed to Paclitaxel had an abnormal network of microtubules around the nucleus at 4–8 h after treatment, which induced the formation of multipolar spindles. Nevertheless, those cells entered G2/M to form a defective spindle–chromosome complex that then caused cycle arrest [22]. Cell proliferation assays indicated that a lower concentration of Paclitaxel was sufficient to induce cell death in comparison to Vincristine [Fig. 2], perhaps, because Paclitaxel did target a higher number of nodes. Fluorescent images from PC-3 cells treated with paclitaxel [Fig. 3A] showed enlarged cells with damaged microtubules and irregular and multiple nuclei suggesting mitotic catastrophe [39]. On the other hand, Vincristine effect on cells was more evident, it resulted in enlarged cells with enlarged and irregular nuclei, and aggregation of compact and denser microtubules around a large nucleus [Fig. 3A and B]. In addition, there was the appearance of some apoptotic cells marked with a red arrowhead [Fig. 3A]; these results correspond with previous findings in several resistant cells lines, which can be ascribed to drug efflux pumps, mutations in tubulin that abrogates drug binding, ineffective interaction with the target, deficient induction of apoptosis and overexpression of prosurvival Bcl-2 family proteins [39,41].

During apoptosis, it is expected the decrease of the anti-apoptotic proteins Bcl-2 like [8,23,24]. However, the overexpression of Bcl-2 and Bcl-xL in PC-3 cells might contribute to the apoptosis-resistant phenotype [42,43]. In this respect, our data indicate that the anti-apoptotic protein Bcl-2 decrease occurred after both treatments, but a portion of the Bcl-2 protein remains in the cells, even after 48 h, contributing to the resistance [Fig. 4A and B]. MTAs initiate the translocation of Bim from microtubules to the mitochondria, allowing the Bax/Bak activation and then inducing apoptosis [12,43]. Nonetheless, the increasing of the pro-apoptotic Bim protein found after both drug treatments, corresponded with several studies in which Bim is reported as a tumor suppressor and is essential for apoptosis induction [26,27,37,44]. Literature reports that Bim level increases dramatically after paclitaxel treatment [12], according to our findings, the level of Bim was higher in vincristine treatment than the level induced by paclitaxel.

The forced expression of Bim increases Paclitaxel-mediated killing of cells expressing an undetectable level of Bim. Conversely, the knockdown of Bim, but not Bcl-2 expression, decreases the susceptibility of tumor cells to Paclitaxel-mediated killing [27]. Similar observations were made using a panel of breast and prostate cancer cell lines [27,43]. Furthermore, it was proven that the depletion of Bim levels prevented paclitaxel-induced Bax and Bak activation [39]. Paclitaxel impairs microtubule function, causes G2/M cell cycle blockade, mitochondria damage, and p53-independent apoptosis. These results established Bim as a critical molecular link between the microtubule toxic agent, Paclitaxel, and apoptosis [27].

Prior to any antineoplastic treatment, Bim is bound by Bcl-2, and there has been proven to be a displacement of Bim from apoptotic proteins consistent with the Paclitaxel treatment at 48 h in four breast cancer cell lines (MCF-7, T47D, MDA-MB-468 and BT20), 3 p53 mutant [43], similar to our findings, where the Bim/Bcl-2 complex level started diminishing at 48 h for both treatments, releasing Bim to initiate apoptosis via Bax/Bak activation [Fig. 5B]. Likewise, the Bim/Bax complex level decreased, indicating that Bim might act as a tumor suppressor that dissociates the anti-apoptotic interaction and promotes Bax release, replacing the p53 function absent in PC-3 cells [37].

Additionally, the levels of the procaspase and the activated form, cleaved-caspase-3 variated significantly indicating that caspase-3 activation during cell death induction in PC-3 cells depends on the drug mechanism. It was shown that Paclitaxel and Vincristine drive the activation of caspase-3 in two breast cells lines, MCF-7 and MDA-MB231, and as it's suggested that those microtubules disrupting agents provoke a signaling cascade and a cellular response to DNA damage [40,45]. The activation of caspase-3 has been considered a remarkable end-point of apoptosis independently of the activated pathway, therefore, the activation of caspase-3 for both treatments is concluded as the induction of apoptosis [Fig. 4B] [46].

Furthermore, new interactions between the cleaved caspase-3 and Bcl-2 or Bim were found, in which, Vincristine interactions seems to increase in a time-dependent manner in both treatments. Contrary to Paclitaxel interactions which decrease also in a time-dependent manner [Fig. 5].

Conclusions

In this study, we reported secondary targets predicted to microtubule-targeting agents, Paclitaxel and Vincristine and we show differences in their effects on PC-3 androgen-independent prostate cancer cells. These are anticancer drugs with a high clinical value that demonstrated noticeable differences in their sensitivities, protein profiles and the protein complex kinetics, confirming that selectivity in the stimulation of the apoptotic system varies depending on the cell's genotype, and the drug exposure period. Thus, they might differ in the formation and quantification of new protein immunocomplexes, such as the one between cleaved-caspase-3 and the pro-apoptotic proteins Bim and Bcl-2.

Conflicts of interest

The authors declare that they have no competing interests.

Acknowledgements

This research was supported by Colciencias and Universidad de Ciencias Aplicadas y Ambientales. Grant number 599-2014. We thank Andrés Gutierrez for the bioinformatics contributions during his stay at the U.D.C.A.

Appendix A. Supplementary data

Supplementary data to this article can be found online at https://doi.org/10.1016/j.bj.2019.04.003.

REFERENCES

[1] Kreeger PK, Lauffenburger DA. Cancer systems biology: a network modeling perspective. Carcinogenesis 2010;31:2–8.
[2] Kann MG. Protein interactions and disease: computational approaches to uncover the etiology of diseases. Brief Bioinform 2007;8:333–46.
[3] Zhang DY, Ye F, Gao L, Liu X, Zhao X, Che Y, et al. Proteomics, pathway array and signaling network-based medicine in cancer. Cell Div 2009;4:4–20.
[4] Guo NL, Wan Y-W. Network-based identification of biomarkers coexpressed with multiple pathways. Cancer Inform 2014;13s5:CIN.S14054.
[5] Gutiérrez-Escobar AJ, Méndez-Callejas G. Interactome analysis of microtubule-targeting agents reveals cytotoxicity bases in normal cells. Genom Proteom Bioinform 2017;15:352–60.
[6] Tai S, Sun Y, Squires JM, Zhan H, Oh WK, Liang CZ, et al. PC3 is a cell line characteristic of prostatic small cell carcinoma. Prostate 2011;71:1668–79.
[7] Lehmann S, Bykov VJN, Ali D, Andrén O, Cherif H, Tidefelt U, et al. Targeting p53 in vivo: a first-in-human study with p53-targeting compound APR-246 in refractory hematologic malignancies and prostate cancer. J Clin Oncol 2012;30:3633–9.
[8] Sobue S, Mizutani N, Aoyama Y, Kawamoto Y, Suzuki M, Nozawa Y, et al. Mechanism of paclitaxel resistance in a human prostate cancer cell line, PC3-PR, and its sensitization by cabazitaxel. Biochem Biophys Res Commun 2016;479:808–13.
[9] The Global Cancer Observatory. Globocan. 2018. http://gco.iarc.fr/. [Accessed 22 February 2019].
[10] Ceresoli GL, Bonomi M, Sauta MG. Chemotherapy. In: Bertoldo B, Boccardo F, Bombardieri E, Evangelista L, Valdagni R, editors. Bone metastases from prostate cancer. Springer; 2017. p. 121–33.
[11] Field JJ, Kanakkanthara A, Miller JH. Microtubule-targeting agents are clinically successful due to both mitotic and interphase impairment of microtubule function. Bioorg Med Chem 2014;22:5050–9.
[12] Bray K, Chen H-Y, Karp CM, May M, Ganesan S, Karantza-Wadsworth V, et al. Bcl-2 modulation to activate apoptosis in prostate cancer. Mol Cancer Res 2009;7:1487–96.
[13] Ceresoli GL, Bonomi M, Sauta MG, Zanardi E, Boccardo F. Combinations of hormonal therapy and chemotherapy. In: Bertoldo B, Boccardo F, Bombardieri E, Evangelista L, Valdagni R, editors. Bone metastases from prostate cancer. Springer; 2017. p. 135–46.
[14] Chen HB, Sun Y, Wu CY, Magyar C, Li XM, Cheng L, et al. Pathogenesis of prostatic small cell carcinoma involves the inactivation of the P53 pathway. Endocr Relat Cancer 2012;19:321–31.
[15] Chappell WH, Lehmann BD, Terrian DM, Abrams SL, Steelman LS, McCubrey JA. p53 expression controls prostate cancer sensitivity to chemotherapy and the MDM2 inhibitor Nutlin-3. Cell Cycle 2012;11:4579–88.
[16] Carroll AG, Voeller HJ, Sugars L, Gelmann EP. p53 oncogene mutations in three human prostate cancer cell lines. Prostate 1993;23:123–34.
[17] Vaseva AV, Moll UM. The mitochondrial p53 pathway. Biochim Biophys Acta 2009;1787:414–20.
[18] De Luca P, Moiola CP, Zalazar F, Gardner K, Vazquez ES, De Siervi A. BRCA1 and p53 regulate critical prostate cancer pathways. 2013. Prostate Cancer Prostatic Dis 2013;16:233–8.
[19] Min KW, Lee SH, Baek SJ. Moonlighting proteins in cancer. Cancer Lett 2016;370:108–16.
[20] Rovini A, Savry A, Braguer D, Carré M. Microtubule-targeted agents: when mitochondria become essential to chemotherapy. Biochim Biophys Acta 2011;1807:679–88.
[21] Kumar N, Salar RK, Prasad M, Ranjan K. Synthesis, characterization and anticancer activity of vincristine loaded folic acid-chitosan conjugated nanoparticles on NCI-H460 non-small cell lung cancer cell line. EJBAS 2018;5:87–99.
[22] Wang C, Huang SB, Yang MC, Lin YT, Chu IH, Shen YN, et al. Combining paclitaxel with ABT-263 has a synergistic effect on paclitaxel resistant prostate cancer cells. PLoS One 2015;10:e0120913.
[23] Yang M-C, Lin R-W, Huang S-B, Huang S-Y, Chen W-J, Wang S, et al. Bim directly antagonizes Bcl-xl in doxorubicin-induced prostate cancer cell apoptosis independently of p53. Cell Cycle 2016;15:394–402.
[24] Yamanaka K, Rocchi P, Miyake H, Fazli L, Vessella B, Zangemeister-Wittke U, et al. A novel antisense oligonucleotide inhibiting several antiapoptotic Bcl-2 family members induces apoptosis and enhances chemosensitivity in androgen-independent human prostate cancer PC3 cells. Mol Cancer Ther 2005;4:1689–98.
[25] Blagosklonny MV, Dixon SC, Figg WD. Efficacy of microtubule-active drugs followed by ketoconazole in human metastatic prostate cancer cell lines. J Urol 2000;163:1022–6.
[26] Blagoskionny MV, Giannakakou P, El-Deiry WS, Kingston DGI, Higgs P, Neckers L, et al. Raf-1/bcl-2 phosphorylation: a step from microtubule damage to cell death. Cancer Res 1997;57:130–7.
[27] Li R, Moudgil T, Ross HJ, Hu H-M. Apoptosis of non-small-cell lung cancer cell lines after paclitaxel treatment involves the BH3-only proapoptotic protein Bim. Cell Death Differ 2005;12:292–303.
[28] Logue SE, Martin SJ. Caspase activation cascades in apoptosis. Biochem Soc Trans 2008;36:1–9.
[29] Winter RN, Kramer A, Borkowski A, Kyprianou N. Loss of caspase-1 and caspase-3 protein expression in human prostate cancer. Cancer Res 2001;61:1227–32.
[30] Szklarczyk D, Santos A, von Mering C, Jensen LJ, Bork P, Kuhn M. STITCH 5: augmenting protein-chemical interaction networks with tissue and affinity data. Nucleic Acids Res 2016;44:380–4.
[31] Shannon P, Markiel A, Ozier O, Baliga NS, Wang JT, Ramage D, et al. Cytoscape: a software environment for integrated models of biomolecular interaction networks. Genome Res 2003;13:2498–504.
[32] Kanehisa M, Goto S, Sato Y, Furumichi M, Tanabe M. KEGG for integration and interpretation of large-scale molecular data sets. Nucleic Acids Res 2012;40:D109–14.
[33] Méndez-Callejas G, Rodríguez-Mayusa J, Riveros-Quiroga M, Mahete-Pinilla K, Torrenegra-Guerrero R. Antiproliferative activity of chloroformic fractions from leaves and inflorescences of Ageratina gracilis. Emir J Food Agric 2017;29:59–68.
[34] Thermo Fisher Scientific. PierceTM BCA protein assay Kit. 2013. https://assets.thermofisher.com/TFS-Assets/LSG/manuals/MAN0011430_Pierce_BCA_Protein_Asy_UG.pdf. [Accessed 22 January 2019].
[35] Bio-Rad. A guide to polyacrylamide gel electrophoresis and detection. 2012. Bulletin 6040 Rev B US/EG 13-0891 0513, http://www.bio-rad.com/webroot/web/pdf/lsr/literature/Bulletin_6040.pdf. [Accessed 28 January 2019].

[36] Thermo Fisher Scientific. Protein gel electrophoresis technical handbook. 2015. https://www.thermofisher.com/content/dam/LifeTech/global/Forms/PDF/protein-gel-electrophoresis-technical-handbook.pdf. [Accessed 28 January 2019].
[37] Méndez-Callejas GM, Leone S, Tanzarella C, Antoccia A. Combretastatin a-4 induces p53 mitochondrial-relocalisation independent-apoptosis in non-small lung cancer cells. Cell Biol Int 2014;38:296–308.
[38] Dumontet C, Jordan MA. Microtubule-binding agents: a dynamic field of cancer therapeutics. Nat Rev Drug Discov 2010;9:790–803.
[39] Mc Gee MM. Targeting the mitotic catastrophe signaling pathway in cancer. Mediat Inflamm 2015:146282.
[40] Sun Q, Chen T, Wang X, Wei X. Taxol induces paraptosis independent of both protein synthesis and MAPK pathway. J Cell Physiol 2010;222:421–32.
[41] Xu X, Lai Y, Hua Z. Apoptosis and apoptotic body: disease message and therapeutic target potentials. Biosci Rep 2019;39:1–17.
[42] Mohammad RM, Muqbil I, Lowe L, Yedjou C, Hsu HY. Broad targeting of resistance to apoptosis in cancer. Semin Cancer Biol 2015;35:S78–103.
[43] Lebedeva I, Rando R, Ojwang J, Cossum P, Stein CA. Bcl-xL in prostate cancer cells: effects of overexpression and Down-Regulation on Chemosensitivity. Clin Cancer Res 2000;60:6052–60.
[44] Kutuk O, Letai A. Displacement of Bim by Bmf and Puma rather than increase in Bim level mediates paclitaxel-induced apoptosis in breast cancer cells. Cell Death Differ 2010;17:1624–35.
[45] Srivastava RK, Srivastava AR, Korsmeyer SJ, Nesterova M, Cho-Chung YS, Longo DL. Involvement of microtubules in the regulation of Bcl2 phosphorylation and apoptosis through cyclic AMP-dependent protein kinase. Mol Cell Biol 1998;18:3509–17.
[46] Cardoso HJ, Vaz CV, Correia S, Fifueira MI, Marques R, Maia C, et al. Paradoxical and contradictory effects of imatinib in two cell line models of hormone-refractory prostate cancer. Prostate 2015;75:923–35.